

ANALYSIS OF TOROIDAL ROTATION DATA FOR THE DIII-D TOKAMAK

H. St. John, U. Stroth,* K.H. Burrell, R. Groebner, J. DeBoo, and P. Gohil

General Atomics, San Diego, California 92138-5608, U.S.A.

*Max Planck Institut für Plasmaphysik, Garching, Federal Republic of Germany

INTRODUCTION

Both poloidal and toroidal rotation are observed during routine neutral beam heating operation of the DIII-D tokamak. Poloidal rotation results and the empirical techniques used to measure toroidal and poloidal rotation speeds are described by Groebner et al.¹ Here we concentrate on the analysis of recent measurements of toroidal rotation made during diverted, H-mode operation of the DIII-D tokamak during co- and counter-neutral beam injection of hydrogen into deuterium plasmas. Similar studies have been previously reported for Doublet III,² ASDEX,³ TFTR,⁴ JET,⁵ and other tokamaks.

Our results are based on numerical inversions using the transport code ONETWO,⁶ modified to account for the radial diffusion of toroidal angular momentum. In its simplest, time-independent form, the momentum equation is

$$\nabla \cdot \left(\bar{\Gamma}_w^\nu + \sum_i \bar{\Gamma}_{w,i}^c \right) = T \quad , \quad (1)$$

where $\bar{\Gamma}_w^\nu$ and $\bar{\Gamma}_{w,i}^c$ are the viscous and convective fluxes. The torque T is similar to the prescription given by Goldston,⁷ neglecting field ripple and radial diffusion of fast ions, but accounting for the neutral charge exchange drag term using neutral speeds determined from the model developed by Burrell.⁸ Inclusion of the above equation in the ONETWO transport prescription induces a coupling to the electron and ion energy equations which is not significant for the results presented here.

RESULTS

Unlike ASDEX⁹ we have not observed significant density peaking during counter injection in DIII-D.¹⁰ However rotation speed profiles do show peaking, with central rotation speeds two to three times as high as similar co-injection discharges, as is obvious from examination of Fig. 1. The increased central rotation speed during counter injection is generally accompanied by reduced rotation speeds over the transport region of the plasma, enhancing the velocity shear (and hence viscous heating) while reducing the stored angular momentum to values closer to co injection discharges. The very low (less than 0.2×10^7 cm/sec) central rotation speeds observed for some of the co-injected high beta discharges is probably associated with MHD activity although low m/n modes were not observed.

Examination of Figs. 2 and 3 reveals that the energy and angular momentum confinement times for co and counter injection are approximately equal with similar dependencies on plasma current and beam heating power. The discharges shown in Fig. 2 have $q_{95} > 3.2$ with the momentum and energy confinement times scaling as previously reported for the energy confinement time during co-injection.¹¹ Although it cannot be supported statistically, the figure suggests that angular momentum confinement may be better for counter-injection at high currents. We do not have the experimental data necessary to resolve this conjecture at the present time but it would be consistent with scalings reported for ASDEX,⁹ where an increase in both energy and momentum confinement times is observed.

The behavior of the angular momentum and energy confinement times as a function of absorbed neutral beam power (P_a) for a range of densities, toroidal fields, and plasma currents is given in Fig. 3. There is some evidence that the energy and momentum confinement for these deuterium H-mode plasmas decreases as P_a increases at low toroidal fields [Fig. 3(a)]. This dependency appears to be largely lost at higher toroidal fields [Fig. 3(a,b,c)], with the momentum confinement time closely tracking the energy confinement time. If there is a difference in scaling for counter-injection, we are unable to resolve it due to the limited data available.

The plasma viscosity for four different discharges is shown in Fig. 4. Agreement between the average thermal energy and momentum diffusivities to the degree shown is considered very good, given the inherent uncertainty in these profiles. We have not plotted the diffusivities out to the plasma edge ($\rho = 1.0$) since complicated edge effects, not accounted for in our analysis, are expected to be dominant there.

The Mattor-Diamond¹² theory of ion temperature gradient driven turbulence predicts that ion thermal and momentum diffusivities are equal when η_i modes are active. Our results show consistency with this theory when the observed η_i is approximately equal to 1.5, as in Fig. 4(a). The remaining cases shown in Fig. 4 fall well outside this range due to the flat density profiles observed during H-mode. In all of the cases investigated we found that the enhancement of the turbulence by the sheared toroidal velocity profile, as predicted in Ref. 12, is an insignificant contribution to the total thermal and momentum diffusivities, even in the high shear counter-injection cases.

CONCLUSION

We obtained angular momentum confinement times in a range from ~ 30 to ~ 120 msec, comparable to energy confinement times and following the same scaling laws. For counter-injection, where peaked rotation profiles with central rotation speeds as high as $\sim 1.3 \times 10^7$ cm/sec have been observed, the angular momentum confinement time is close to the values for co-injection at the same absorbed power. The angular momentum diffusivity is found to be in good agreement with the average of the ion plus electron thermal diffusivities.

Evaluation of η_i indicates that ion temperature gradient-driven turbulence is expected to be active, perhaps explaining the equality of thermal and momentum diffusivities. However, most cases investigated to date have η_i values significantly larger than the critical value ($\eta_i^c \approx 1.5$ or $\frac{L_{T_i}}{R} \approx 0.2$) so that direct comparison with experimental data was not possible using our time independent analysis technique. Further investigations using time dependent threshold models developed by Dominguez and Waltz¹³ will be made in the future.

This work was supported by U.S. Department of Energy Contract No. DE-AC03-89ER51114.

REFERENCES

- Groebner, R.J., Gohil, P., Burrell, K.H., Osborne, T.H., Seraydarian, R.P., St. John, H., this conference.
- Burrell, K.H., *et al.*, Nuclear Fusion **28**, 1988 (3).
- Roberts, D.E., *et al.*, 15th European Conference on Controlled Fusion and Plasma Heating, Dubrovnik, May 16, 1988, p. 15.
- Scott, S.D., *et al.*, *ibid.*, p. 103.
- Hawkes, N.I., *et al.*, *ibid.*, P. 1061.
- Pfeiffer, W.W., *et al.*, General Atomics Report GA-A16178, December 1980.
- Goldston, R.J., Proceedings of Course and Workshop: Basic Physical Processes of Toroidal Plasmas (Varenna, 1985) p. 165.
- Burrell, K.H., J. Comp. Phys. **27** (19768) P. 88.
- Fussmann, G., *et al.*, Twelfth International Conference on Plasma Physics and Controlled Nuclear Fusion Research, IAEA, Nice, France, October 1988, IAEA-CN-50/A-3-1.
- Schissel, D.P., *et al.*, General Atomics Report GA-A19503, December 1988.
- Schissel, D.P., *et al.*, General Atomics Report GA-A19243, February 1988.
- Mattor, N., Diamond, D.H., Phys. Fluids **31**, (1988) p. 1180.
- Dominguez, R., and Waltz, R., General Atomics Report GA-A19342, November 1988.

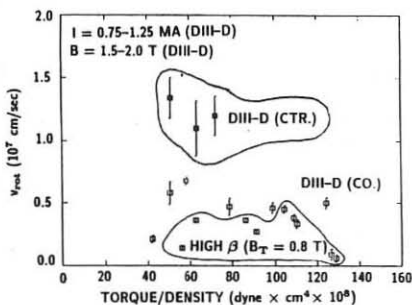


Fig. 1. Central rotation versus torque per ion/ m^3

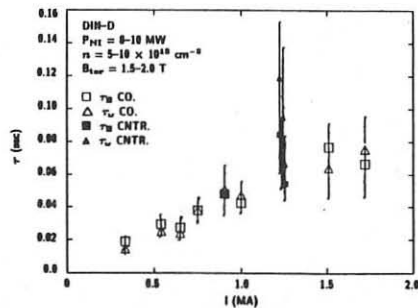


Fig. 2. Energy and momentum confinement time versus plasma current

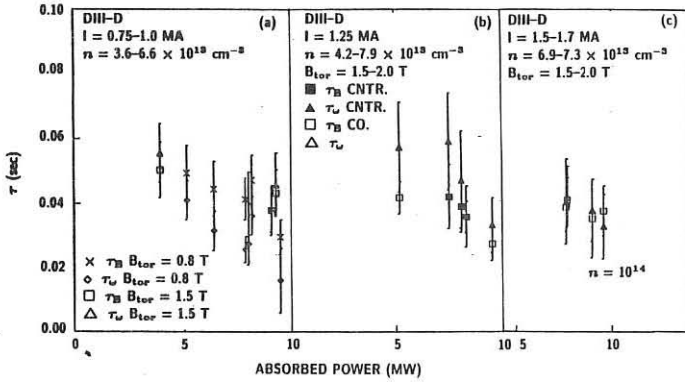


Fig. 3. Energy and momentum confinement time versus absorbed power

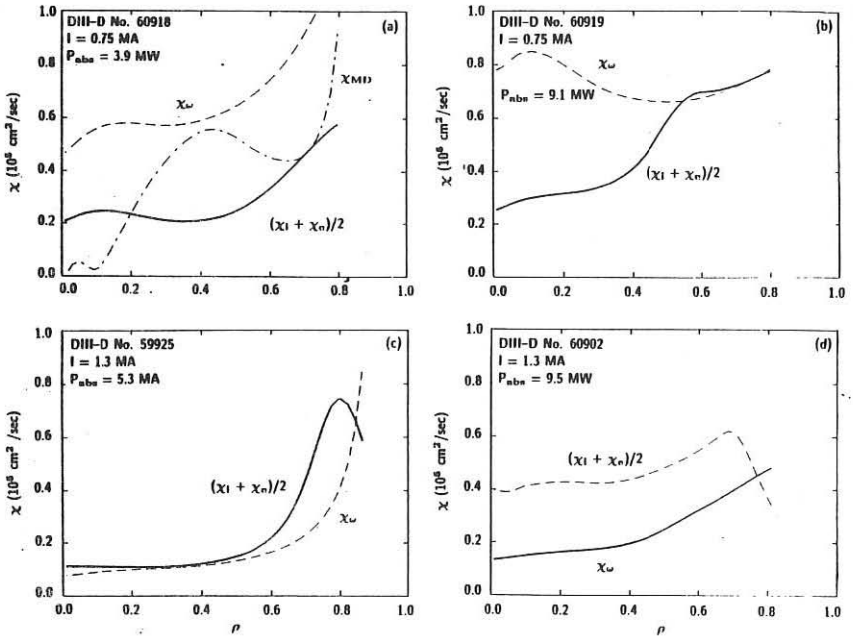


Fig. 4. Comparison of thermal and momentum diffusivities.